Advances in Volcanology

Rise and fall of a multi-sheet intrusive complex, Elba Island, Italy

--Manuscript Draft--

Manuscript Number:	AVOL-D-13-00004R1
Full Title:	Rise and fall of a multi-sheet intrusive complex, Elba Island, Italy
Article Type:	Physical Geology of Shallow Magmatic Systems
Abstract:	The western Elba igneous system is a prime example of a full range of emplacement styles at a single magmatic center, with successive generation of a nested set of multi-layer laccoliths, a downward-developing amalgamated pluton, an extensive throughgoing dyke swarm, with a final collapse of the whole complex triggered by the overwhelming thickness of magma added to the uppermost crust in a short time.
Corresponding Author:	Sergio Rocchi Università di Pisa Pisa, ITALY
Corresponding Author Secondary Information:	
Corresponding Author's Institution:	Università di Pisa
Corresponding Author's Secondary Institution:	
First Author:	David Scott Westerman
First Author Secondary Information:	
Order of Authors:	David Scott Westerman
	Sergio Rocchi
	Andrea Dini
	Federico Farina
	Emanuele Roni
Order of Authors Secondary Information:	
Author Comments:	

Rise and fall of a multi-sheet intrusive complex, Elba Island, Italy

Westerman D.S.[1], Rocchi S.[2], Dini A.[3], Farina F.[4], Roni E.[2]

1. Department of Geology, Norwich University, Northfield, Vermont, USA
2. Dipartimento di Scienze della Terra, Università di Pisa, Pisa, Italy
3. Istituto di Geoscienze e Georisorse, CNR (Consiglio Nazionale delle Ricerche), Pisa, Italy
4. Departamento de Geologia, Universidade Federal de Ouro Preto, Minas Gerais, Brasil

1 Introduction

Elba Island is the site of a prime example of a very young igneous complex including multiple multisheet laccoliths, a sheeted pluton and an extensive dyke swarm, all emplaced at the same location in about 1.5 Ma. Elba Island is located at the northern end of the Tyrrhenian Sea, a region affected by extensional processes leading to the opening of an ensialic back-arc basin behind the eastward progressing compressive front of the Apennine mobile belt (Malinverno and Ryan 1986).

The structural framework of Elba Island (Fig. 1) developed during the Apenninic compressional event before 20 Ma, which led to the stacking of five major tectonic complexes on east-verging thrusts. The three lowest complexes (I-III) have continental features consisting of metamorphic basement and shallow-water clastic and carbonate rocks, while the upper two complexes (IV-V) have oceanic characteristics: Complex IV consists of Jurassic oceanic lithosphere of the western Tethys Ocean (peridotite, gabbro, pillow basalt and ophiolite sedimentary breccia) and its late Jurassic – middle Cretaceous sedimentary cover (chert, limestone, and argillite interbedded with siliceous limestone); Complex V consists mostly of an upper Cretaceous siliciclastic turbidite sequence (Pertusati et al. 1993). This stacking of tectonic complexes on top of the Apennine fold-and-thrust belt is characterized by a large number of physical discontinuities such as thrust contacts between tectonic complexes and bedding planes within the turbidite sequence of Complex V.

After 20 Ma, compression continued, but the stalled subduction transformed to an eastward-migrating slab rollback and lithospheric delamination of the Adriatic plate (Serri et al. 1993). Asthenosphere rose against the base of the middle-upper crust, became partially molten by decompression, and generated uplift and extension of the crust, heat transfer, and ultimately anatectic melting of crustal materials. In turn, extensional tectonics produced low- and high-angle normal faults, adding physical discontinuities to the stacked Tuscan tectonic complexes.

In this framework, magmas were generated in the crust and in the mantle, leading to the variety of intrusive and extrusive products of the Tuscan Magmatic Province exposed across an area of about 30,000 km^2 of southern Tuscany and the northern Tyrrhenian Sea. This igneous activity migrated from west (14 Ma) to east (0.2 Ma) (Serri et al., 1993).

Igneous activity in western-central Elba Island (Tuscany) led to the emplacement of several magma bodies over a time span of about 1.5 Ma during the Late Miocene, with the relative chronology of all units firmly established on the basis of consistent crosscutting relations. The igneous sequence can be subdivided into three main events: (1) the construction of three multilayer laccoliths, first by the emplacement of the layers of Capo Bianco aplite, followed in succession by the layers of the Portoferraio laccolith and finally, the San Martino laccolith (Rocchi et al. 2002); (2) intrusion and/or deformation of the deepest laccolith layers by the Monte Capanne

pluton and its associated late leucocratic dykes and veins (Farina et al. 2010); (3) emplacement of the mafic Orano dyke swarm, cutting through the entire succession (Dini et al. 2008). Absolute ages, noted subsequently, are consistent with the relative chronology constrained by field relations.

Shortly after the intrusive sequence was assembled, the upper part of the igneous-sedimentary system was tectonically translated eastward along the low-angle Central Elba Fault (Fig. 1). Following this eastward translation, a "west side up" movement occurred along the high-angle Eastern Border Fault (Fig. 1) with a throw of 2 to 3 km so that the lower part of the sequence is presently exposed in western Elba at the same level as the upper part in central Elba (Westerman et al. 2004). This process, coupled with nearly 100% coastal exposure on the island, led to the serendipitous exposure of a 5-km-thick crustal section including nine intrusive layers of late Miocene age that built up three multilayer Christmas-tree laccoliths.

2 The intrusive sheets (multilayer laccoliths)

2.1 Christmas tree geometry of the laccolith complex

Magmatism in Elba was initiated with emplacement at c. 8.5 Ma of the Capo Bianco aplite, a bony white rock, so unique that it is also reported in ancient Greek myths (Dini et al. 2007). This unit is found in two layers, within tectonic Complexes IV and V (Fig. 1): the lower layer is preserved as caps on ridges with a minimum thickness of 50 meters, while the upper horizon crops out along the north coast of central Elba with a minimum thickness of 120 meters. Mineralogy includes microphenocrysts of sanidine, plagioclase and muscovite, with significant amounts of tourmaline occurring as dark blue orbicules (Dini et al. 2007). Intrusive contacts are very rare for the Capo Bianco aplite, seen only locally against flysch of Complex V. Elsewhere, the stratigraphic and tectonic thrust surfaces along which Capo Bianco magma intruded also served as the loci for magma injection during the next episode of magmatism. This resulted in the remaining Capo Bianco aplite material being entirely encased in younger laccolith horizons. Calculated minimum volume for the Capo Bianco system is 0.63 km^3, and can be thought of as the crust “breaking a sweat” of anatectic melt generated by muscovite dehydration melting, setting the stage for arrival of a much larger volume of magma derived by a higher degree (muscovite and biotite involved), and much greater amount, of melting in the source area (Dini et al. 2002).

This second episode of magmatism led to the emplacement, at c. 8 Ma, of the Portoferraio porphyry at the same magmatic center, ultimately occupying four major horizons with two thin sheets (75 m) and one thick sheet (700 m) in Complex IV, and another thick sheet (400 m) in the flysch sequence of Complex V (Figs. 2 and 4). These porphyries are characterized by sanidine phenocrysts typically averaging 1 to 2 cm (Fig. 3a). Quartz and biotite phenocrysts are ubiquitous, all set in a very fine-grained matrix predominantly made of quartz and K-feldspar.

The third and final episode of laccolith emplacement occurred following a delay in magmatic activity of approximately 0.6 Ma. It was marked by the arrival of the very distinctive San Martino porphyry characterized by prominent euhedral decimetric megacrysts of sanidine (Fig. 3c). These megacrysts are accompanied by remarkable amounts of quartz, plagioclase and biotite phenocrysts, all suspended in a very fine-grained isotropic groundmass of quartz and feldspars, with mafic microgranular enclaves generally present as well (Dini et al. 2002). With the exception of a principal feeder dyke located in western Elba (Fig. 1), the three main horizons of the San Martino laccolith are currently located in central Elba where they were translated by the tectonic-gravitational decapitation of the complex (Figs. 2 and 4). Two lower

horizons (100-200 m thick) occur beneath the main 700-meter thick sheet that has a reconstructed diameter of nearly10 km (Fig. 5) (Rocchi et al. 2002); the emplacement sequence for these three sheets is unresolved.

2.2 Magma flow in the laccolith

One aspect of the study of laccoliths involves developing insight to processes of magmatic flow associated with the feeding and filling of such bodies. The San Martino laccolith system (Fig. 5) lends itself very well to this type of work owing to the ubiquitous presence of euhedral sanidine megacrysts, and platy biotite phenocrysts, which can reveal the occurrence of a fabric via attitude measurements or via AMS analysis (anisotropy of the magnetic susceptibility), respectively. A combined analysis of megacryst orientations and AMS fabric (Roni et al. 2014) demonstrated a strong correlation between orientations of megacrysts and magnetic fabric, strengthening the use of AMS as magma strain indicator. It further suggests that: (i) the lack of post-emplacement tectonic deformation, as well as the fast cooling of the shallow igneous system, the quick emplacement, and the high magma viscosity, permit direct correlation between strain in the rock and magma flow, (ii) a central dyke with sub-vertical flow fed the main laccolith horizons, (iii) magma spreading laterally from the feeding system built the laccolith layers as single propagating and inflating pulses, in which the planar surfaces of particles became aligned perpendicular to the magma displacement direction (Fig. 6) in an inferred divergent flow field (Paterson et al., 1995), and (iv) the absence of internal discontinuities agrees with the hypothesis of continuous feeding of the magma injected as a single pulse or a series of pulses that quickly coalesced, confirming rapid emplacement of the body.

2.3 Laccolith growth

Excellent exposure and significant 3-D relief has allowed detailed mapping leading to reconstruction of the geometries of nested multi-layered laccoliths on Elba, with each lithologically recognizable laccolith consisting of a set of individual sheets with measured thicknesses and diameters (Rocchi et al. 2002). The dimensional parameters of these intrusive layers fit a power-law distribution (Fig. 7) indicating that, after a likely first stage of horizontal expansion, the layers underwent a second stage of dominantly vertical inflation (Rocchi et al. 2002). It is worth noting that, once the layers of the Portoferraio and San Martino laccolithic layers are virtually merged as two single intrusive bodies and plotted again in the length vs. thickness diagram, they plot on the fit lines proposed for plutons (Cruden and McCaffrey 2002) (Fig. 7). This evidence shows that, if the laccolith sheets had coalesced, they would have ended up as two plutons having aspect ratios compatible with both (i) the power-law fit curves for plutons worldwide (McCaffrey and Petford 1997; Cruden and McCaffrey 2001) and (ii) the S-type fit curve proposed for all intrusive bodies (Cruden and McCaffrey 2002). Taken together, the laccoliths from Elba can be seen as sheet-like intrusions that did not coalesce to form single laccoliths or plutons.

2.4 Laccolith emplacement

The observation that the laccolith failed to coalesce to form a composite pluton but emplaced as separate sheets in a Christmas tree geometry raises questions regarding the mechanisms governing the emplacement of shallow level granitic intrusions. Each magma batch created its own room by lifting the rock overburden, indicating that the magma driving pressure was greater than the vertical stress (Hogan et al. 1998; Kerr and Pollard 1998). These conditions provide evidence that crustal magma traps arrested the vertical ascent of Elba magmas (Hogan and Gilbert

1995; Hogan et al. 1998). A significant control on the ascent of Elba magma by magma driving pressure is supported by the aspect ratios of all the Elba intrusions (i.e. their overall tabular shapes), coupled with the occurrence of vertical dykes below the subhorizontal sheets, indicating that magma ascent at Elba occurred through feeder dykes that likely remained connected to the magma reservoir (Brown and Solar 1998; Dehls et al. 1998; Hogan et al. 1998). The magma driving pressure is

$$P_d = P_h + P_0 - P_{vis} - S_h$$

(Reches and Fink 1988; Baer and Reches 1991; Hogan and Gilbert 1995; Hogan et al. 1998), where P_h is the hydrostatic pressure, P_0 is the magma chamber overpressure, P_{vis} is the viscous pressure drop, and S_h is the horizontal stress, i.e. perpendicular to the ascending dyke walls. In the case of the Elba magmas, the magma chamber overpressure can be considered negligible due to the low volatile contents, and the viscous pressure drop is of little influence when values of 0.5 MPa km^{-1} are adopted (Baer and Reches 1991; Hogan et al. 1998). The hydrostatic pressure, defined as the difference between the lithostatic pressure at the top of the magma reservoir (i.e. at the source depth) and the pressure at the tip of the column of magma as it rises through the crust (Hogan and Gilbert 1995) can be calculated at any depth based on the knowledge of the depth of the magma source, the integrated density of the crust overlying the magma source, and the integrated density of the rising magma (Rocchi et al. 2010). The horizontal stress is the sum of the lithostatic load and the tectonic stress, which is a function of the regional state of crustal stress. In late Miocene time, the upper crust at Elba was in a tensional stress regime, and all the intrusions were emplaced within the two uppermost Apennine tectonic units, i.e. in the brittle crust (Rocchi et al. 2010).

All the Elba magma batches project a positive driving pressure value at the surface, thus having the potential to erupt (Fig. 8), yet, to our knowledge, none of them did so. The only known volcaniclastic material in the late Miocene sediments in mainland Tuscany has an isotopic age (7.4 Ma) comparable to that of the San Martino laccolith, yet its mineral and chemical features correlate this material to the volcanic activity of Capraia Island (Rocchi et al. 2010). The two main laccolith units were emplaced at depths shallower than where the ascending magma driving pressure first exceeded the vertical stress. The Portoferraio laccolith layers were emplaced on a set of available physical discontinuities in a depth zone only slightly shallower than that point, that is the magma switched from vertical to horizontal movement as soon as the magma left behind the densest host rock unit (the ophiolite sequence) and acquired the ability to lift the overburden (i.e. driving pressure exceeds vertical stress; Fig. 8a). Furthermore, a prominent physical discontinuity occurred at that depth, namely the thrust surface between tectonic complexes IV and V. The San Martino magma layers were emplaced in a zone some 1000 m above the Portoferraio laccolith layers, in that the younger magma was able to ascend higher than the previous batch. It switched from vertical to horizontal propagation and had the ability to lift the overburden when it met a set of crustal magma traps (Fig. 8b), i.e. the physical discontinuities within the turbidite sequence (competence contrast between sandstone and shaly layers, plus internal thrusts).

3 The sheeted intrusion (pluton)

3.1 Internal structure of the Monte Capanne pluton

Western Elba is dominated by the Monte Capanne pluton with its nearly circular map pattern and impressive relief as it rises 1 km out of the sea. Formal study of the

geology of Elba has gone on for more than two centuries, fueling controversy on both absolute and relative ages of the porphyries and the granite pluton (Dini et al. 2009). The Monte Capanne pluton is now recognized as consisting of three distinct facies (Fig. 3d, f), despite the absence of mappable internal contacts between them, emplaced at 6.9 Ma (Dini et al. 2002). Common characteristics of the three facies include a monzogranitic composition with variable proportions of plagioclase, K-feldspar (commonly as large megacrysts), quartz, and biotite, and the occurrence of mafic microgranular enclaves, displaying strongly variable size and composition (Dini et al., 2002; Farina et al., 2010). Detailed mapping, along with petrographic and geochemical analyses (Farina et al. 2010) indicate that these three facies represent three subhorizontal sheets sequentially emplaced by underplating as discrete magma batches (Fig. 9). Radiometric dating has not yet substantiated the emplacement sequence, and arguments rely primarily on i) the absence of feeding structures to the uppermost, highly distinctive Sant'Andrea facies, despite excellent field exposures (Farina et al. 2010), and ii) emplacement of increasingly more mafic facies (from Sant'Andrea to San Piero facies) following the overall temporal trend of progressive increase of mantle contribution to the magmas as reported for all of western-central Elba magmatism (Dini et al., 2002). The total thickness of the pluton has been estimated at ~2.5 km using magnetic data (Dini et al. 2008). Rocks of the Sant'Andrea facies are preserved along the pluton margin and at high elevations, and are characterized by the highest SiO_2 content, highest biotite Mg#, highest K-feldspar megacryst content (area % is 3.37 ± 0.56 (1σ), corresponding to ~57 megacrysts/m^2), and highest mafic microgranular enclaves content. The facies exposed at the deepest levels is the San Piero facies, which has opposing characteristics (area % is 0.26 ± 0.21 (1σ); ~4 megacrysts/m^2), while rocks of the San Francesco facies are intermediate both in character and in spatial distribution (Fig. 9). The process of stepwise emplacement of the pluton deformed the surrounding host rocks while metamorphosing them, resulting in flattening of its thermal aureole with mylonitization of the deepest porphyry layers of the Portoferraio laccolith (Fig. 3b).

3.2 Sheet growth and pluton build-up

The reconstructed original dimensional parameters of the three intrusive sheets making up the Monte Capanne pluton (Farina et al. 2010) display a power-law correlation that, in analogy with the laccolith layers, can be interpreted as indicative of a similar vertical inflation stage in the sheet growth history (Fig. 7), such that both the multilayer laccoliths and the sheeted pluton formed in a "laccolithic" way.

When the dimensional parameters of the Monte Capanne pluton as a whole (i.e. the result of the amalgamation of three sheets in a single intrusive body) are plotted in the length-thickness diagram, they fit those predicted for plutons worldwide (McCaffrey and Petford 1997; Cruden and McCaffrey 2001; Cruden and McCaffrey 2002). In summary, the magma batches forming the pluton did amalgamate in a single, composite intrusive body, while the amalgamation was not possible for the laccolith sheets since they were emplaced on multiple surfaces separated by intercalating host rocks and ""frozen" in their vertical inflation stage (Rocchi et al. 2010).

3.3 Magma sheet emplacement

The sequence of events that led to formation of an amalgamated pluton such as the Monte Capanne pluton, rather than a set of discrete sheets such as Portoferraio and San Martino laccoliths, has significant implications for our understanding of magma emplacement mechanisms in the upper crust (Rocchi et al. 2010).

The first magma batch of the Monte Capanne pluton (Sant'Andrea sheet) was emplaced deeper than the laccoliths, at about 6 km, but its petrochemical features do not differ enough from those of the San Martino magma to explain such a difference in emplacement level. Therefore, there is no straightforward explanation why the ~8 Ma and the ~7.4 Ma magma batches were emplaced at depths of less than 3 km as separated intrusive sheets with aphanitic groundmass, whereas the three ~7 Ma magma batches did, in fact, coalesce at a deeper level to form a single, coarse-grained intrusive body. A plausible explanation is linked to the combined occurrence of (i) magma source deepening as a direct consequence of the addition of ~ 2.4 km of porphyry to the uppermost crust, and (ii) increase of the magma supply rate, as suggested by the abundant mafic microgranular enclaves of metric size in the Sant'Andrea magma batch (Westerman et al. 2003). The inferred increase in rate of supply and resulting dilational stress gave way to a transient reduction of the horizontal stress (Hogan and Gilbert 1995), possibly supplemented by ongoing slab roll-back. In this context, a stress reduction of about 40% is enough to cause an increase in magma driving pressure (Fig. 8c, magenta dashed line) sufficient to overcome the vertical stress at a depth corresponding to the emplacement depth of the Sant'Andrea magma pulse (Rocchi et al. 2010). This batch of magma thus emplaced as a rather thin (250 m) sheet, very rich in K-feldspar megacrysts, large quartz phenocrysts and large mafic microgranular enclaves. The following San Francesco magma batch was emplaced below the Sant'Andrea sheet, with the cryptic nature of the contact between the two facies suggesting that the second one was emplaced at the base of a mushy tabular body (Saint-Blanquat et al. 2006; Farina et al. 2010). Such mushy bodies are natural traps for ascending batches of magma (Brown 2007) because they generate a rigidity anisotropy that triggers horizontal expansion of subsequent magma batches (Menand 2008) and growth of the intrusion by under-accretion. A similar history was repeated on the arrival of the third (San Piero) magma batch that was emplaced at the base of the San Francesco sheet.

The remarkable increase in matrix grain size from laccoliths to pluton is a consequence of the more extended crystallization history of the pluton's magma batches. This is, in turn, linked to the greater depth of the pluton's magma trap in two ways: (i) the higher temperature of the crust at the depth of pluton emplacement results in a slower crystallization, and (ii) the slightly higher depth of emplacement, at such low pressures (< 200 MPa), may result in significant increase in water solubility, depression of solidus temperature, and more extended crystallization temperature range, all leading to a coarser-grained matrix (Hogan et al. 2000). This extended crystallization can also help explain the cryptic nature of the contacts between facies of the pluton. Taken together, all three pulses of magma were assembled in a downward stack by exploiting traps of their own making, thus building a "successful" pluton. This is contrasted with the slightly older multisheet laccoliths located above (Fig. 7), which exploited pre-existing structural traps and, therefore, could be seen as a "failed" pluton. Additionally, progressive warming of the crust during magma emplacement throughout growth of the entire igneous complex is also suggested by the increasing evidence of mafic magma intruding the crust, as seen from the growing amount of mafic enclaves through time, and the emplacement of the late mafic Orano magma (Dini et al., 2002).

3.4 Plutons vs. laccoliths

The shape, emplacement and assembly history of the Monte Capanne intrusion raises questions as to which category of intrusive bodies it belongs. For its medium- to coarse-grained texture and emplacement depth, Monte Capanne has been classically regarded as a pluton. Nevertheless, it could also be regarded as a sheeted laccolith that was emplaced deeper than the normal depth limit of about 3

km, and slightly exceeded the ca. 2 km limiting thickness owing to the rapid removal of the roof by tectonic-gravitational collapse. However, more important than its classification is the understanding that at Elba Island, similar magma batches in similar settings resulted in intrusive bodies that significantly differ in their shape, texture and emplacement depth.

As a take-home lesson, in an upper crust characterized by abundant magma traps, the failed (laccolith) or successful (pluton) assembly of magma batches can thus be linked to different outcomes of the same geological process operating under different transient conditions. The transition from a laccolithic to a plutonic intrusive shape having a higher thickness-to-diameter ratio can be governed by a combination of factors such as variations in rates of magma supply and horizontal extensional tectonic stress, as well as downward migration of both the source region and the magma traps as a result of the addition of magma layers at higher levels in the crust.

4 The dyke swarm

4.1 Geometry of the Orano dykes

More than 200 individual dykes with cumulate length in excess of 90 km were emplaced 6.85 Ma mostly in the northwestern half of the still not completely solidified Monte Capanne pluton (Figs. 1 and 10) and, more limitedly, in its covering laccolith layers (Fig. 1) (Dini et al. 2008). These dark dykes (Fig. 3g), are porphyritic, with plagioclase, biotite, clinopyroxene and amphibole phenocrysts set in a very fine-grained matrix of plagioclase, K-feldspar and phlogopite. Some dykes, generally the thickest, are zoned with borders similar to unzoned dykes, and inner portions reaching monzogranitic compositions owing to the incorporation of abundant quartz and K-feldspar xenocrysts (Fig. 3h) from the still mushy Monte Capanne magmatic system. The original melt derived from a specific mantle source with geochemical–isotopic characteristics intermediate between Capraia K-andesites and Tuscan lamproites (Dini et al. 2002).

Vertical expression of the dykes exceeds 4 km, ranging from sea level exposures in the Monte Capanne pluton, upward through the exposed thickness of the pluton, and finally through the entire exposed cover sequence tectonically translated to the east and now preserved in central Elba. The dykes were probably fed by a mafic magma reservoir located below the northwestern half of the Monte Capanne pluton, as suggested by magnetic data (Dini et al. 2008). The dykes reveal an organized structural pattern with a dominant system made of one set trending ENE, and a minor system consisting of two sets trending NNE and NW (Fig. 11). Analysis of the structural patterns in conjunction with established tectonic conditions at the time of emplacement of the dyke swarm suggests that they developed in a NE-SW dextral shear zone within which zones of differential strain created local zones of sinistral shear (Dini et al. 2008). It is interesting to note that an overall N-S extensional stress field apparently persisting at this location from the time of emplacement of the San Martino laccolith system with its E-W feeder system, through emplacement of the Monte Capanne plutonic complex, and into emplacement of the Orano dyke swarm.

4.2 Insight to the regional geology

Emplacement of the Orano dyke swarm closed a ~1.5 Ma long episode of magmatism located at a single center and fed by sources from both the crust and underlying mantle. This final stage in the development of the entire igneous complex, with the high degree of hybridization and xenocryst capture, documents that a late-plutonic dyke swarm can intrude before complete consolidation of its host. The

Orano dyke swarm offers further evidence for a regionally significant implication that magmatic activity in the late Miocene occurred within a transfer zone in the northern Tyrrhenian region. However, as important as the sequence of igneous activity is, its cessation at an individual center also carries significance. Regional patterns of magmatism in the Tuscan Magmatic Province shows how that transfer zone structure, and perhaps others aligned parallel to it, served as a "fire line" along which magmatism migrated northeastward producing a trace of progressively younger magmatic centers (Dini et al. 2008).

5 Post-magmatic evolution: the structural failure

5.1 Collapse of the magmatic edifice

The rocks comprising western Elba prior to the magmatism discussed above had been assembled as a stack of eastward-directed thrusts of bedded sedimentary rocks above an ocean lithosphere sequence. In approximately 1 Ma, this 2.7 km thick tectonostratigraphic section was inflated by the addition of a total of 2.4 km of intrusive layers (Rocchi et al. 2002) in a roughly circular region with a diameter of approximately 10 km located over a common magmatic center (Fig. 12). The primary crustal magma trap for the first half of that magmatism was the well-defined top of the Complex IV ophiolite sequence beneath the overlying Complex V flysch sequence. This structure was located at the middle of the newly thickened section that defined a domal structure with a new slope of about 25° (Westerman et al. 2004).

As pulses of Monte Capanne magma approached the base of Complex IV, adding an additional estimated 2.5-3 km of new rock under the laccolith intrusions (Dini et al. 2008), the slopes would have steepened (Fig. 12). The system held in place throughout emplacement of the Monte Capanne pluton and long enough for the Orano dyke swarm to be injected throughout the whole vertical section. Ultimately, however, the Complex IV/V boundary ultimately failed and triggered the catastrophic eastward tectonic-gravitational décollement on the Central Elba Fault that transported the top “half” of the laccolith units about 8 km to the east over a < 1.5 Ma period, with a rate of displacement in excess of 5-6 mm/a (Fig. 12) (Westerman et al. 2004). This combination of (i) loading central Elba with several km of igneous rock, and (ii) the unweighting of western Elba by the removal of that rock, promoted the development of the Eastern Border Fault, with back-tilting of the central Elba stack to the east and uplift of the unroofed western Elba rocks to the west. This ultimately achieved 3 to 4 km of normal movement on a steep, eastward-dipping surface.

5.2 A lesson from destruction

The story of the “fall of western Elba” (Westerman et al. 2004), illustrates how basic geological relationships can document geologic history on a grand scale. The onset of major movement on the Central Elba Fault is constrained by fragments of the Monte Capanne contact aureole (~6.9 Ma) in the footwall mélange located at least 8 km east of the pluton, along with the translation of the upper portion of the slightly younger Orano dyke swarm. Constraint on the termination of the major displacement is also provided with simple geologic relations, as cobbles of western Elba lithologies from below the fault are found in conglomerates deposited close to the end of the Messinian (~5.3 Ma) about 50 km away on mainland Italy (Pandeli et al. 2010).

These relationships suggest that gravity-assisted fast sliding (5-6 mm a^{-1}) of a 2.5 km-thick crustal slice decapitated western Elba (Westerman et al. 2004). This activity would undoubtedly have been associated with numerous seismic events over of an extended period, and awareness of such possibilities should be incorporated into hazard assessment of highly over-steeped magmatic centers. As a final implication of this entire body of work, there is simply be no substitute for detailed mapping coupled with the tools from all branches of geology.

6 Conclusions

The western Elba igneous system serves as a prime example of a full range of emplacement styles at a long-lasting magmatic center, with successive generation of a nested set of multi-layer laccoliths, a downward-developing amalgamated pluton, an extensive throughgoing dyke swarm, with a final collapse of the whole complex triggered by the overwhelming thickness of magma added to the uppermost crust in a short time.

Pre-existing structures provide strong constraints on emplacement style, and resulted in very similar magmas producing both porphyritic as well as granitic (plutonic) textures. The Elba laccolith sheets failed to coalesce and form a larger pluton/laccolith with typical dimensions due to the availability of a large number of magma traps in the host crust that consists of a thrust stack of well-layered rocks. On the other hand, the three magma pulses of the Monte Capanne pluton were assembled in a downward stack, building a “successful” pluton as opposed to the “failed” plutons represented by the multi-sheet laccoliths. Also possible is the opposite view that regards the Monte Capanne pluton as a “failed” laccolith, as opposed to the “successful” multilayer laccoliths of Portoferraio and San Martino.

In the upper crust, laccoliths and plutons represent different outcomes of the same process in different settings. The "tipping point" allowing for transition from a laccolithic to a plutonic intrusive shape is controlled by factors such as variabilities of magma supply rate and horizontal tectonic stress, as well as by downward migration of the source region and/or the magma traps as a result of the progressive addition of magma at higher crustal levels. Also the rate of magma addition to the crust dramatically increased corresponding to the emplacement of the Monte Capanne pluton (Fig. 13). Although magma emplaced in pulses separated by quiescence gaps, it can be noticed that during the laccolith events, the long-term rate of magma production, ascent and accumulation in the shallow crust was around 50 km^3/Ma, while around 7 Ma, the Monte Capanne and the mafic Orano episodes, magma was produced at an accelerated rate ten to twenty times higher. Reasons for this boost can be linked to the increased production of mafic melt acting as an additional heat source promoting the shift of the crustal melt-producing reactions from muscovite-biotite breakdown to the more productive biotite-hornblende breakdown (Dini et al. 2002; Farina et al. submitted). Finally, the addition of excess magma at a unique igneous center in a short time span can trigger gravity slides displacing km-thick slices of crust by several kilometers at geologically fast rates.

List of Figures

Figure 1. Simplified geological map of western and central Elba Island. In the inset, the hatched line represents the present front of the Apennine-Maghrebide and Alpine chains.

Figure 2. Geological map of the western-central Elba laccolith layers draped over a digital elevation model. View from the south. Scale varies in perspective view.

Figure 3. (a) Portoferraio porphyry, with sanidine phenocrysts up to 2 cm long; hammer for scale. (b) Foliated Portoferraio porphyry, 1.5 km NW of Marciana; the foliation is N52W, 55N (parallel to the local contact with the Monte Capanne pluton) with stretching lineation 50, N5E, pointing out a genetic link between pluton emplacement and deformation; width of the field of view: 15 cm. (c) San Martino porphyry, eastern side of Marina di Campo Bay, showing abundant aligned sanidine megacrysts in relief (width of field of view: 1.6 m). (d) Megacryst-rich Sant'Andrea facies of the Monte Capanne pluton, Sant'Andrea shore; note the euhedral shapes of megacrysts (as opposed to those in the San Piero facies) and the coarse-grained matrix (as opposed to the San Martino porphyry); notebook for scale is 20 cm-long. (e) Megacryst- and mafic microgranular enclave-rich Sant'Andrea facies, Sant'Andrea shore. (f) Megacryst-poor San Piero facies of the Monte Capanne pluton, abandoned quarry close to Seccheto; hammer for scale. (g) Typical Orano dyke within Monte Capanne granite, close to Chiessi; hammer for scale. (h) Orano dyke (left) in contact with Monte Capanne granite (right); note the dyke contains xenocrysts of quartz with ocellar texture and of K-feldspars with rounded shape; coin for scale.

Figure 4. Geological cross-sections of the western-central Elba laccolith units.

Figure 5. Schematic representation of the San Martino multilayer laccolith, superimposed on a field photo of the laccolith layers cropping out on the cliffs east of Marina di Campo Bay (width of photo is ~1 km).

Figure 6. Magmatic flow pattern in the San Martino laccolith based on poles of restored magmatic and magnetic foliations projected on the current map pattern. Dashed blue line trending E-W marks separation of N and S halves of the main laccolith layer, with the west end representing the approximate eastern terminus of the Marciana feeder dyke system. The upper-left inset depicts the relationships between magma flow (red arrows) and the orientation of the platy K-feldspar and biotite crystals (Roni et al. 2014).

Figure 7. Log-log plot of T vs. L (T = thickness; L = diameter of sheets). The general power-law equation describing the relationships between L and T has the form $L = kT^a$ (where k is a constant and a is the slope of a regression line in a log-log plot. Dimensional data for laccoliths from (Rocchi et al. 2002) and for Monte Capanne pluton sheets from (Farina et al. 2010). Fit lines for plutons and laccoliths from McCaffrey and Petford (1997) and Cruden and McCaffrey (2001); bold violet S-type fit line for all intrusive bodies from Cruden and McCaffrey (2002). The grey balls represent the L-T values for virtually amalgamated laccoliths and the naturally amalgamated pluton: laccolith values calculated from total thickness and average diameter; pluton value from all sheets naturally amalgamated as a result of the intrusion process. The number inside each grey ball indicates the intrusion volume (in km^3).

Figure 8. Variations in magma driving pressure ($P_d = P_h + P_0 - P_{vis} - S_h$; see text), magma pressure ($P_m = P_h + P_0 - P_{vis} - S_v$) and vertical stress ($S_v=\rho gh$, where ρ=integrated crustal density, g=gravity acceleration, h=depth) as a function of depth for (a) Portoferraio laccolith magma, (b) San Martino laccolith magma, and (c) the Sant'Andrea sheet magma, the first magma batch of the Monte Capanne pluton; magenta dashed line corresponds to increased magma driving pressure resulting from a 40% horizontal stress reduction. Each curve is constructed according to

Hogan and Gilbert (1995) and Hogan et al. (1998) using published crustal density profiles for Elba (Rocchi et al. 2010).

Figure 9. Geological map of area% of K-feldspar megacrysts, translated to intrusive facies of the Monte Capanne pluton draped over a digital elevation model. Data for map construction after Farina et al. (2010). View from the south. Scale varies in perspective view.

Figure 10. Geological map of the Orano dyke swarm draped over a digital elevation model, view from the SW. The Pomonte-Procchio (PP) line, bordering the SE margin of the outcrop area of Orano dykes, is also reported.

Figure 11. Rose diagrams of the strike of dykes (see maps in Figs. 1 and 10) for zones dominated by the major and minor systems, respectively. Each 10 m section of the 90 km of dykes mapped in the swarm generated a strike value, producing the ~9,000 data points making up the two rose diagrams (from Dini et al. 2008). The diagram on the right has a radius scaled 4x with respect to the one on the left to emphasize the strike distribution within the minor system.

Figure 12. Rise and fall of the western Elba laccolith-pluton-dyke complex: a schematic summary. (a) Emplacement of the Capo Bianco laccolith layers. (b) Emplacement of the Portoferraio laccolith layers. (c) Emplacement of the San Martino laccolith layers. (d) Emplacement of the Sant'Andrea, San Francesco and San Piero magma batches (as sheets building the Monte Capanne pluton from the top down), closely followed by the emplacement of the Orano mafic dyke swarm in the north-western part of the pluton. (e) Décollement of the upper part of the nested laccolith-pluton-dyke complex, with translation to central Elba and unroofing of the Monte Capanne pluton.

Figure 13. Plot of the cumulative volume of the western-central Elba intrusions through time. The volumes of each of the three laccoliths have been determined layer by layer (Rocchi et al. 2002), but they are represented here as a single dot per laccolith since the emplacement sequence of the different layers within the same multilayer laccolith cannot be discerned. On the other hand, the Monte Capanne pluton is represented by three dots based on the emplacement sequence and lags between pulse emplacement reported by Farina et al. (2010). The volume of the Orano swarm has been calculated by adding the estimated total volume of the mapped dykes to the volume inferred for the mafic reservoir located below the northwestern Monte Capanne pluton (Dini et al. 2008).

References

Baer G, Reches Z (1991) Mechanics of emplacement and tectonic implications of the Ramon dike systems, Israel. J Geophys Res 96: 11,895-11,910

Brown M (2007) Crustal melting and melt extraction, ascent and emplacement in orogens: mechanisms and consequences. J Geol Soc, London 164: 709-730

Brown M, Solar GS (1998) Granite ascent and emplacement during contractional deformation in convergent orogens. J Struct Geol 20: 1365-1393

Cruden A, McCaffrey K (2002) Different scaling laws for sills, laccoliths and plutons: mechanical thresholds on roof lifting and floor depression. In: Breitkreuz C, Mock A, Petford N (eds) Physical Geology of Subvolcanic Systems - Laccolith, Sills and Dykes (LASI), Freiberg, 12-14 October 2002, 15-17

Cruden AR, McCaffrey KJW (2001) Growth of plutons by floor subsidence: implications for rates of emplacement, intrusion spacing and melt-extraction mechanisms. Phys Chem Earth 26: 303-315

Dehls JF, Cruden, A R, Vigneresse JL (1998) Fracture control of late Archean pluton emplacement in the northern Slave Province, Canada. J Struct Geol 20: 1145-1154

Dini A, Corretti A, Innocenti F, Rocchi S, Westerman DS (2007) Sooty sweat stains or tourmaline spots? The Argonauts on the Island of Elba (Tuscany) and the spread of Greek trading in the Mediterranean Sea. In: Piccardi L, Masse WB (eds) Myth and Geology, Geological Society, Special Publications, 273, London, 227-243

Dini A, Innocenti F, Rocchi S, Tonarini S, Westerman DS (2002) The magmatic evolution of the laccolith-pluton-dyke complex of Elba Island, Italy. Geol Mag 139: 257-279

Dini A, Rocchi S, Westerman DS, Farina F (2009) The late Miocene intrusive complex of Elba Island: two centuries of studies from Savi to Innocenti. Acta Vulcanologica 20/21: 11-32

Dini A, Westerman DS, Innnocenti F, Rocchi S (2008) Magma emplacement in a transfer zone: the Miocene mafic Orano dyke swarm of Elba Island (Tuscany). In: Thomson K, Petford N (eds) Structure and Emplacement of High-Level Magmatic Systems, Geological Society, London, Special Publication 302, 131-148

Farina F, Dini A, Innocenti F, Rocchi S, Westerman DS (2010) Rapid incremental assembly of the Monte Capanne pluton (Elba Island, Tuscany) by downward stacking of magma sheets. Geol Soc Am Bull 122: 1463-1479

Farina F, Dini A, Rocchi S, Stevens G (submitted) Extreme mineral-scale Sr isotope heterogeneity in granites by disequilibrium melting of the crust

Hogan JP, Gilbert MC (1995) The A-type Mount Scott Granite sheet: importance of crustal magma traps. J Geophys Res B8: 15,779-715,792

Hogan JP, Gilbert MC, Price JD (2000) Crystallisation of fine- and coarse-grained A-type granite sheets of the Southern Oklahoma Aulacogen, U.S.A. Trans Royal Soc Edimburgh: Earth Sci 91: 139-150

Hogan JP, Price JD, Gilbert MC (1998) Magma traps and driving pressure: consequences for pluton shape and emplacement in an extensional regime. J Struct Geol 20: 1155-1168

Kerr AD, Pollard DD (1998) Toward more realistic formulations for the analysis of laccoliths. J Struct Geol 20: 1783-1793

Malinverno A, Ryan WBF (1986) Extension in the Tyrrhenian Sea and shortening in the Apennines as result of arc migration driven by sinking of the lithosphere. Tectonics 5: 227-245

McCaffrey KJW, Petford N (1997) Are granitic intrusion scale invariant? J Geol Soc, London 154: 1-4

Menand T (2008) The mechanics and dynamics of sills in layered elastic rocks and their implications for the growth of laccoliths and other igneous complexes. Earth Planet Sci Lett 267: 93-99

Pandeli E, Bartolini C, Dini A, Antolini E (2010) New data on the paleogeography of Southern Tuscany (Italy) since Late Miocene time. Int J Earth Sci 99: 1357-1381

Paterson, SR, Fowler Jr, TK, Schmidt, KL, Yoshinobu, AS, Yuan, ES and Miller, RB (1998), Interpreting magmatic fabric patterns in plutons. Lithos 44:53-82.

Pertusati PC, Raggi G, Ricci CA, Duranti S, Palmeri R (1993) Evoluzione post-collisionale dell'Elba centro-orientale. Mem Soc Geol It 49: 297-312

Reches Z, Fink J (1988) The Mechanism of Intrusion of the Inyo Dike, Long Valley Caldera, California. J Geophys Res 93: 4321–4334

Rocchi S, Westerman DS, Dini A, Farina F (2010) Intrusive sheets and sheeted intrusions at Elba Island (Italy). Geosphere 6: 225-236

Rocchi S, Westerman DS, Dini A, Innocenti F, Tonarini S (2002) Two-stage laccolith growth at Elba Island (Italy). Geology 30: 983-986

Roni E, Westerman DS, Dini A, Stevenson C, Rocchi S (2014) Feeding and growth of a dyke-laccolith system (Elba Island, Italy) from AMS and mineral fabric data. J Geol Soc, London.

Saint-Blanquat Md, Habert G, Horsman E, Morgan SS, Tikoff B, Launeau P, Gleizes G (2006) Mechanisms and duration of non-tectonically assisted magma emplacement in the upper crust: The Black Mesa pluton, Henry Mountains, Utah. Tectonophys 428: 1-31

Serri G, Innocenti F, Manetti P (1993) Geochemical and petrological evidence of the subduction of delaminated Adriatic continental lithosphere in the genesis of the Neogene-Quaternary magmatism of central Italy. Tectonophys 223: 117-147

Westerman DS, Dini A, Innocenti F, Rocchi S (2003) When and where did hybridization occur? The case of the Monte Capanne pluton. Atlantic Geol 39: 147-162

Westerman DS, Dini A, Innocenti F, Rocchi S (2004) Rise and fall of a nested Christmas-tree laccolith complex, Elba Island, Italy. In: Breitkreuz C, Petford N (eds) Physical Geology of High-Level Magmatic Systems, Geological Society, London, Special Publication 234, 195-213

Figure 1
Click here to download high resolution image

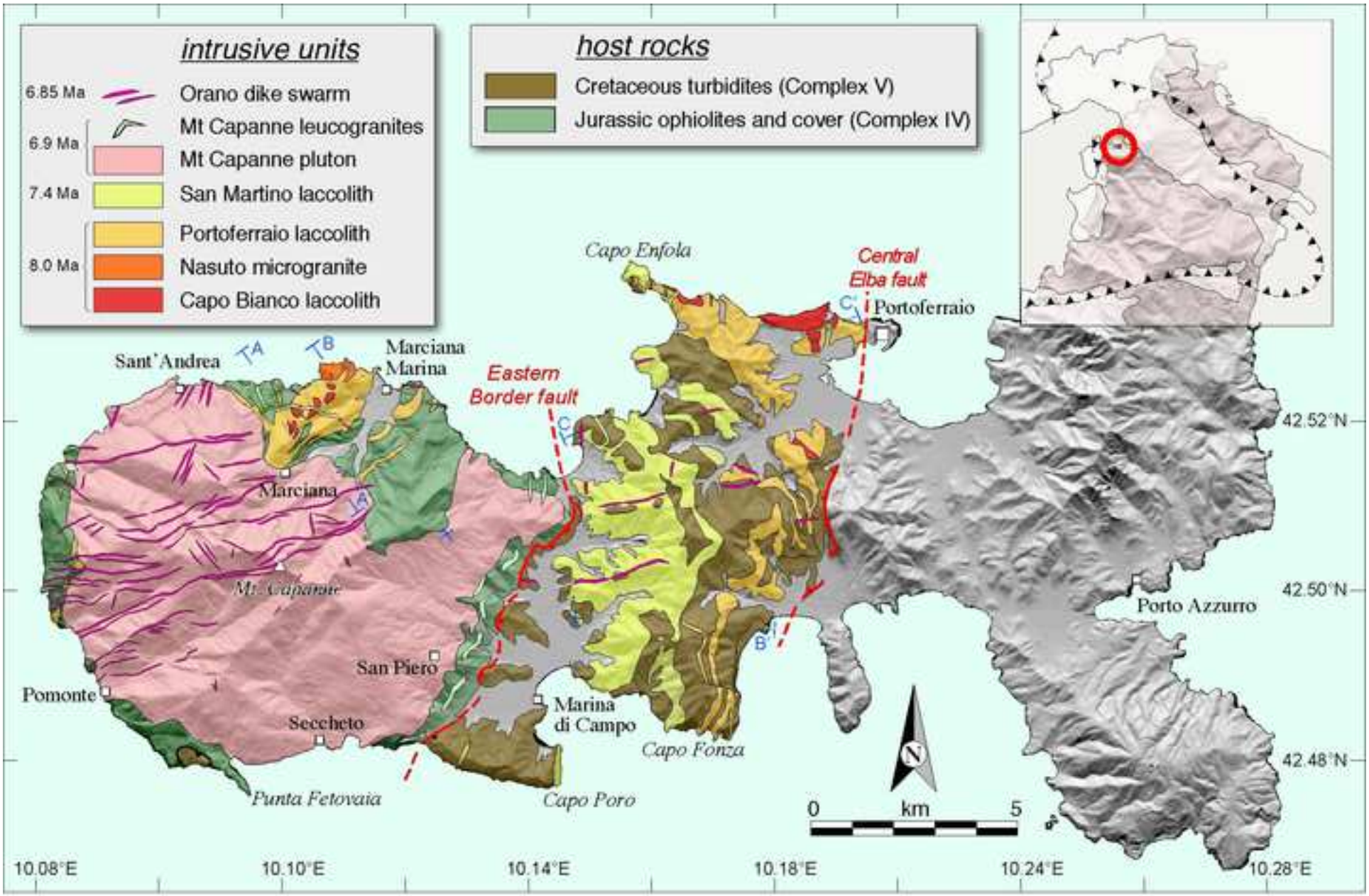

Figure 1

Figure 2
Click here to download high resolution image

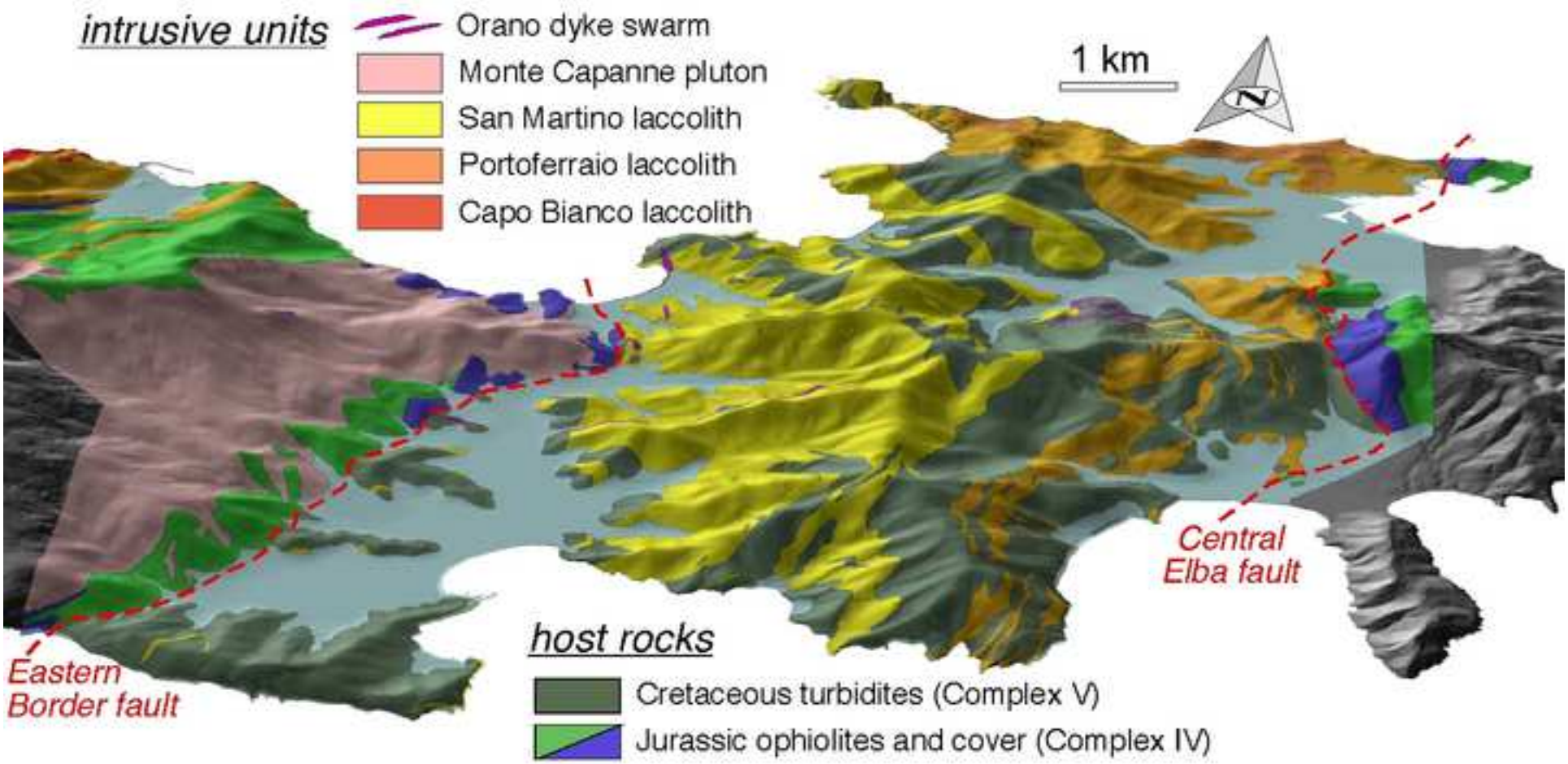

Figure 3
Click here to download high resolution image

Figure 4
Click here to download high resolution image

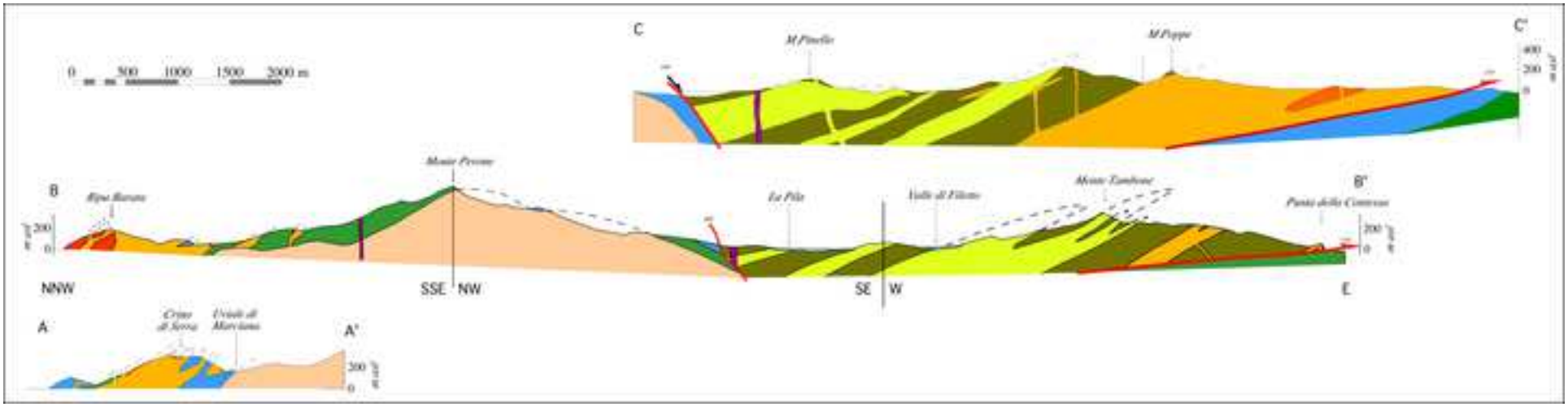

Figure 5
Click here to download high resolution image

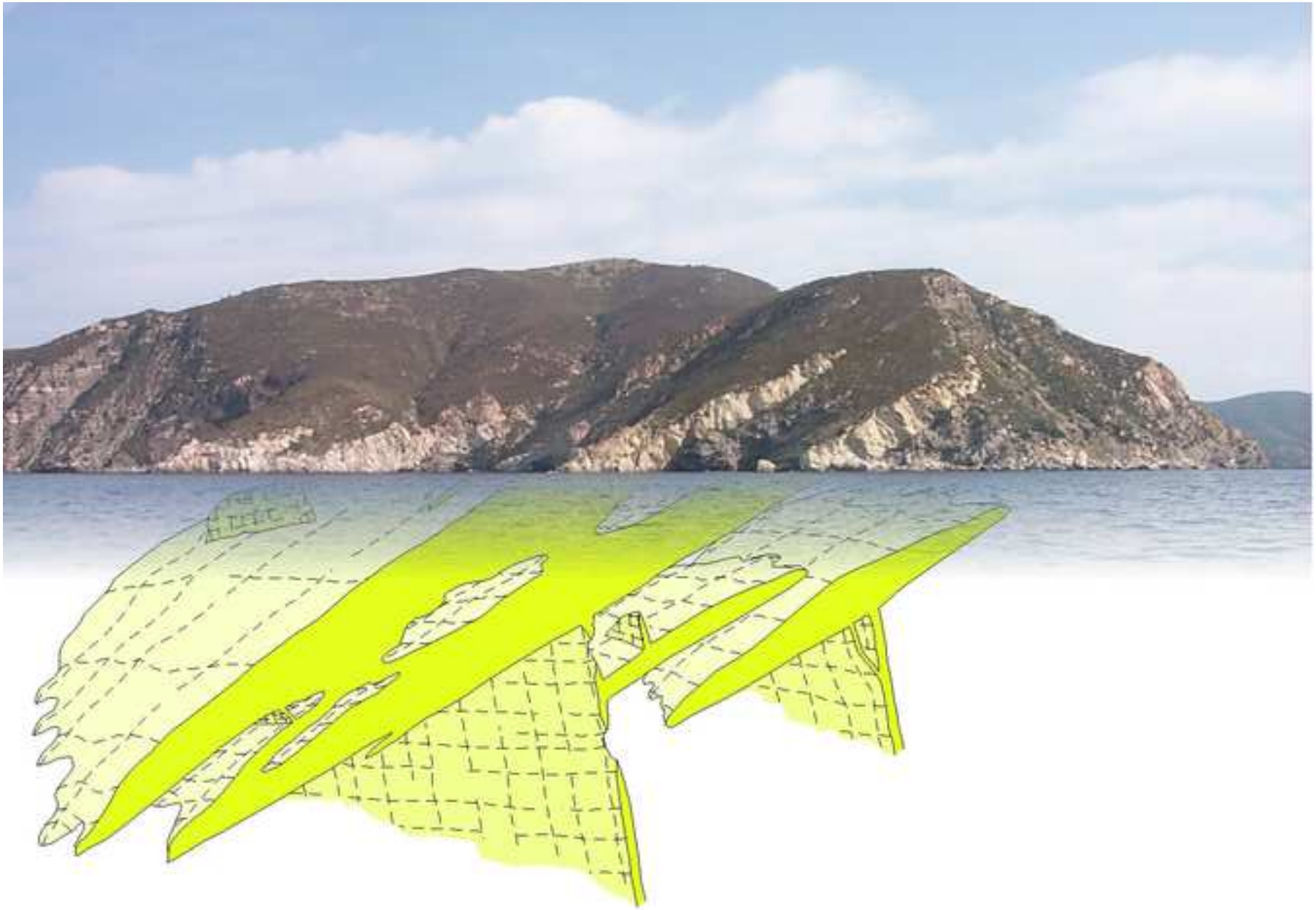

Figure 6
Click here to download high resolution image

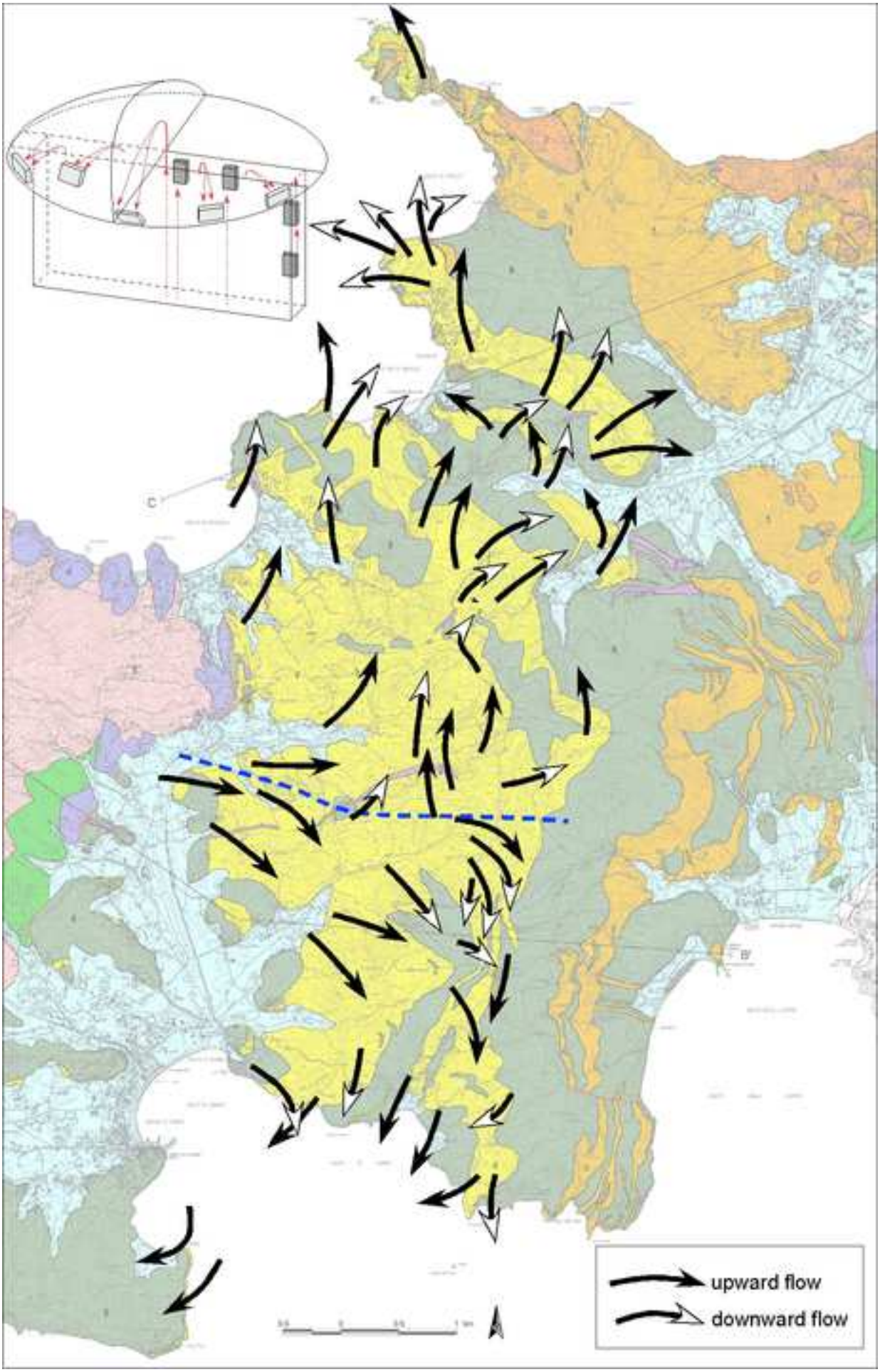

Figure 7
Click here to download high resolution image

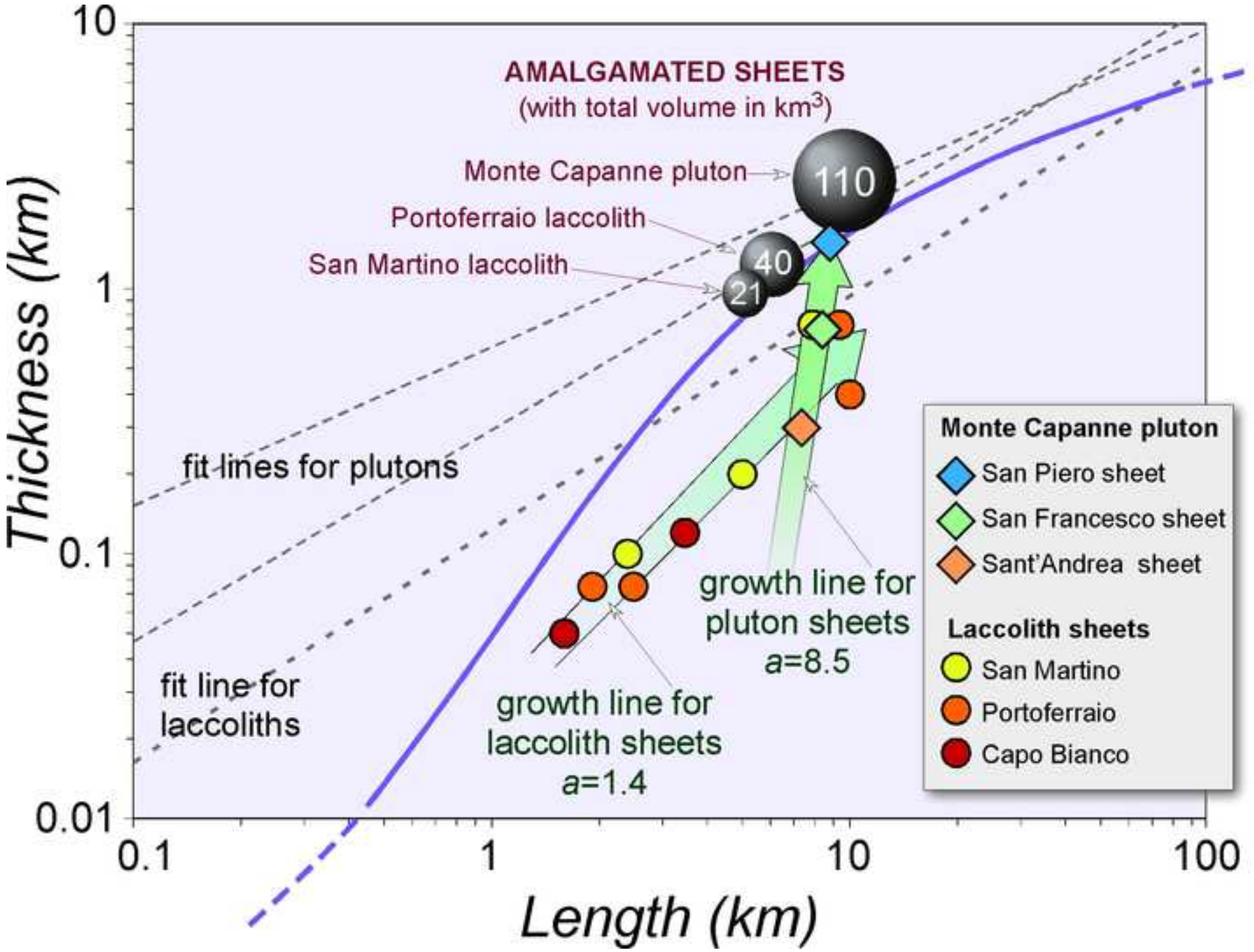

Figure 8
Click here to download high resolution image

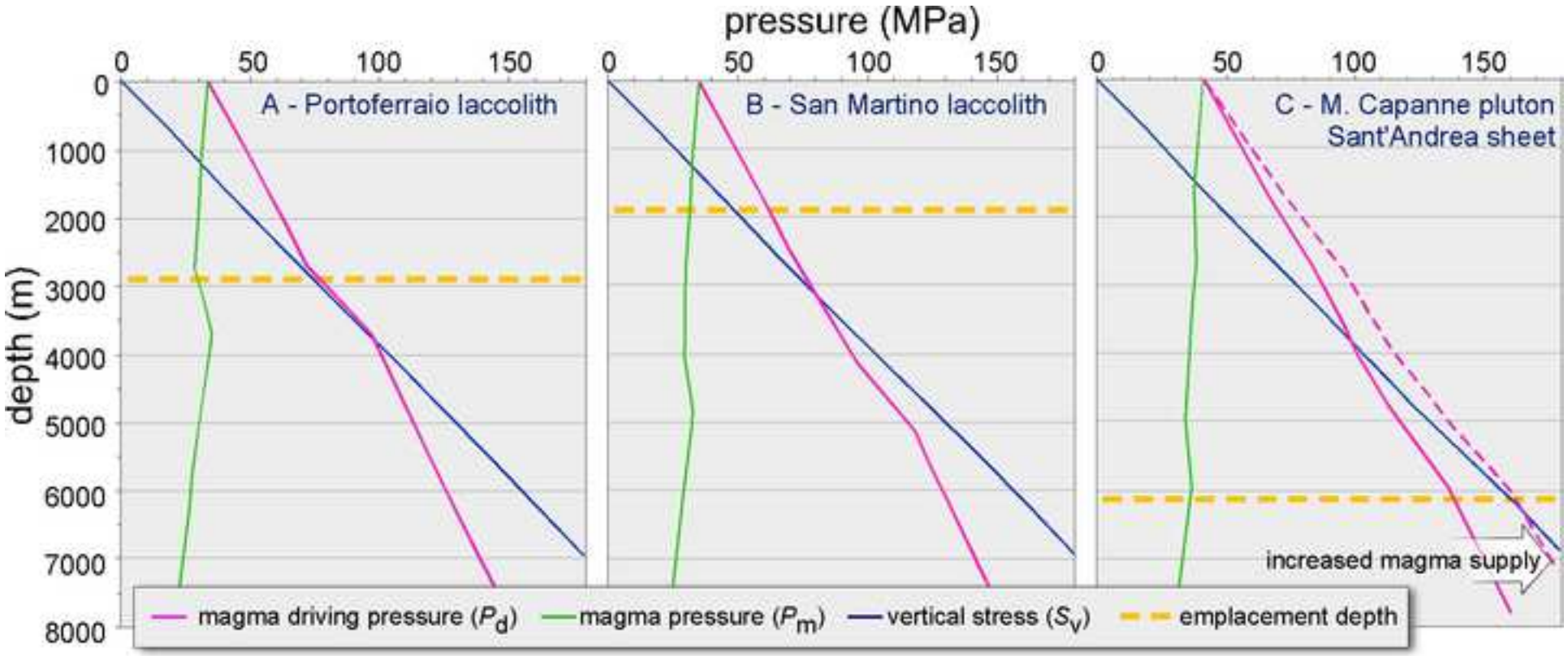

Figure 9
Click here to download high resolution image

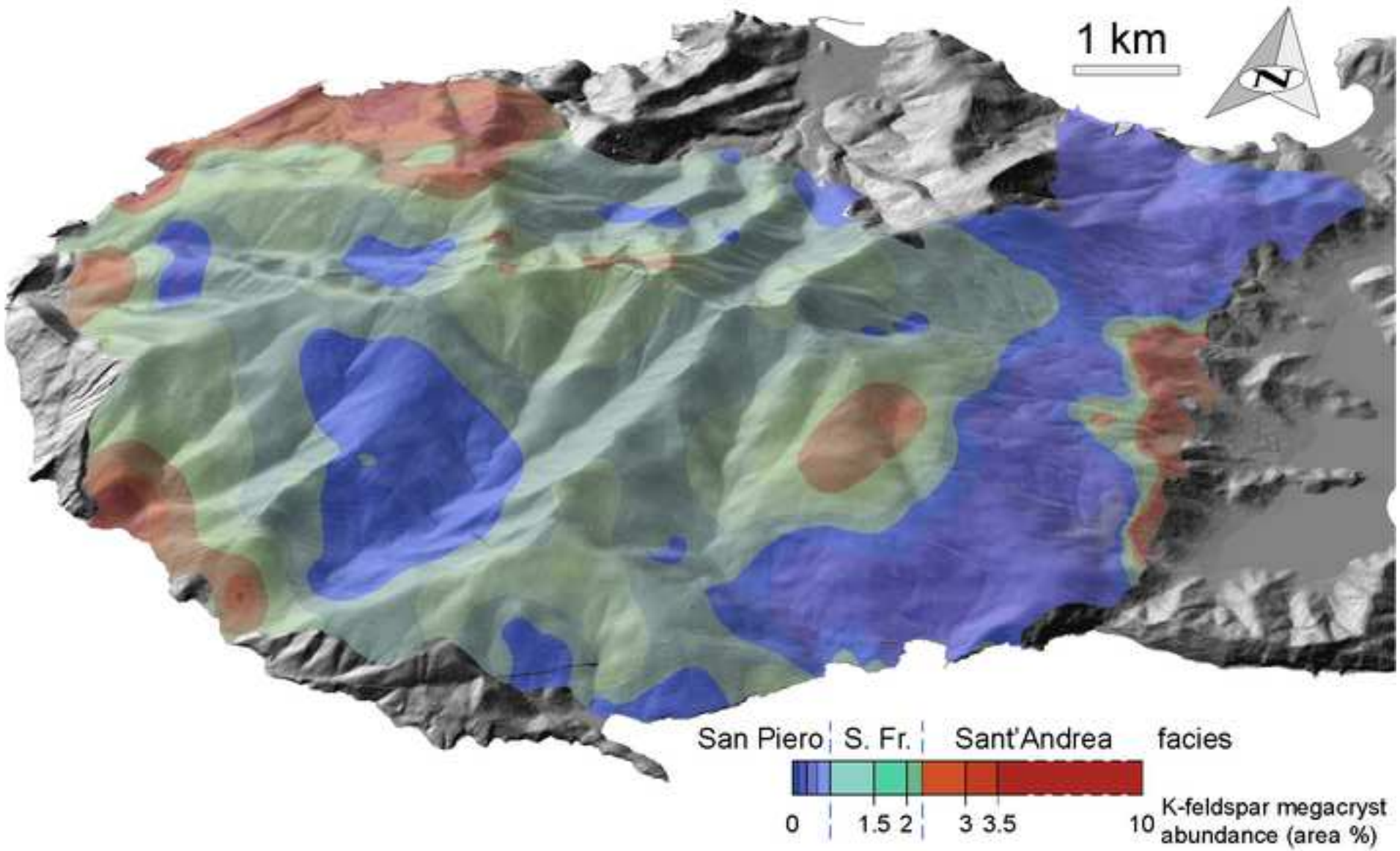

Figure 10
Click here to download high resolution image

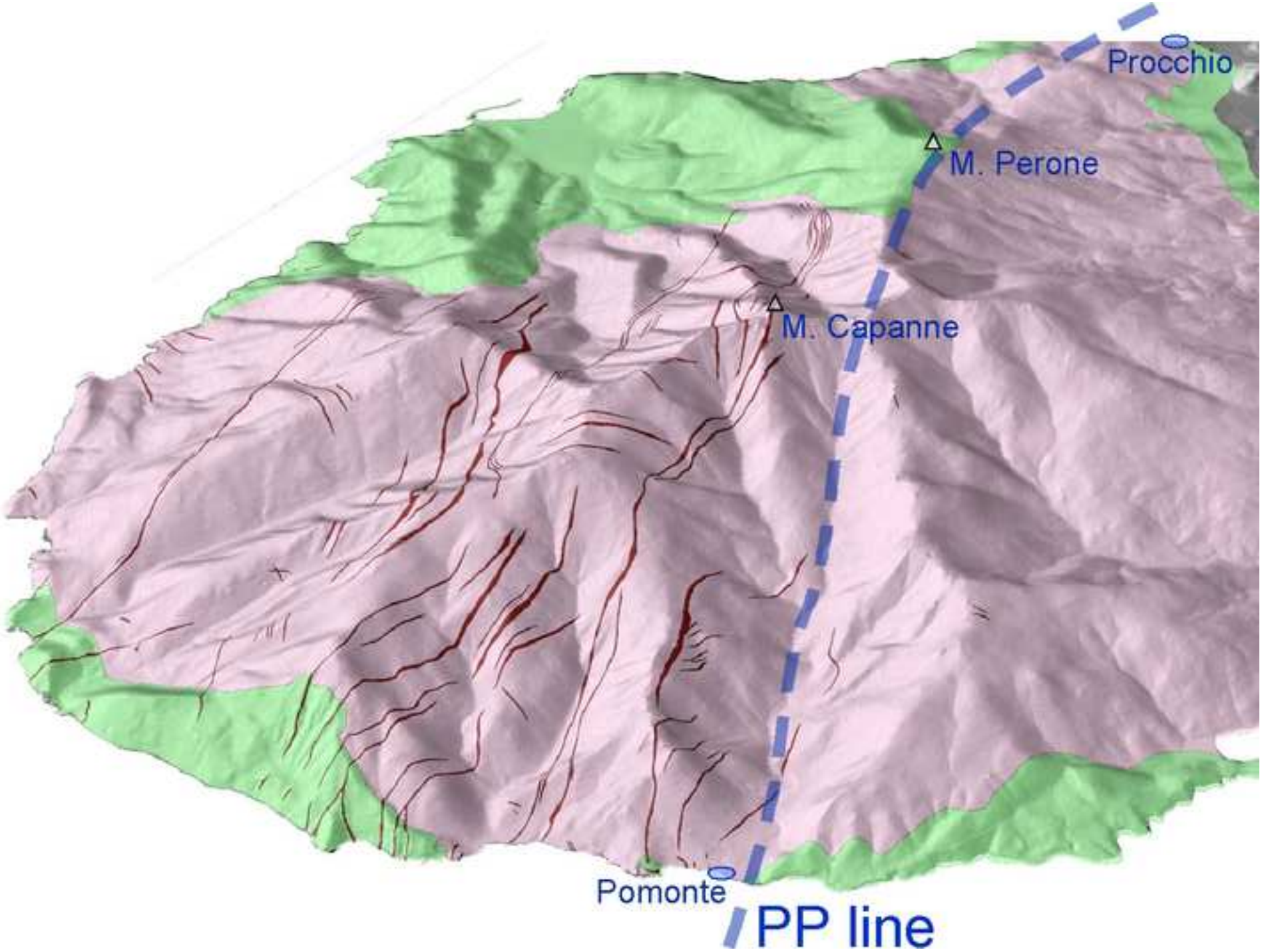

Figure 11
Click here to download high resolution image

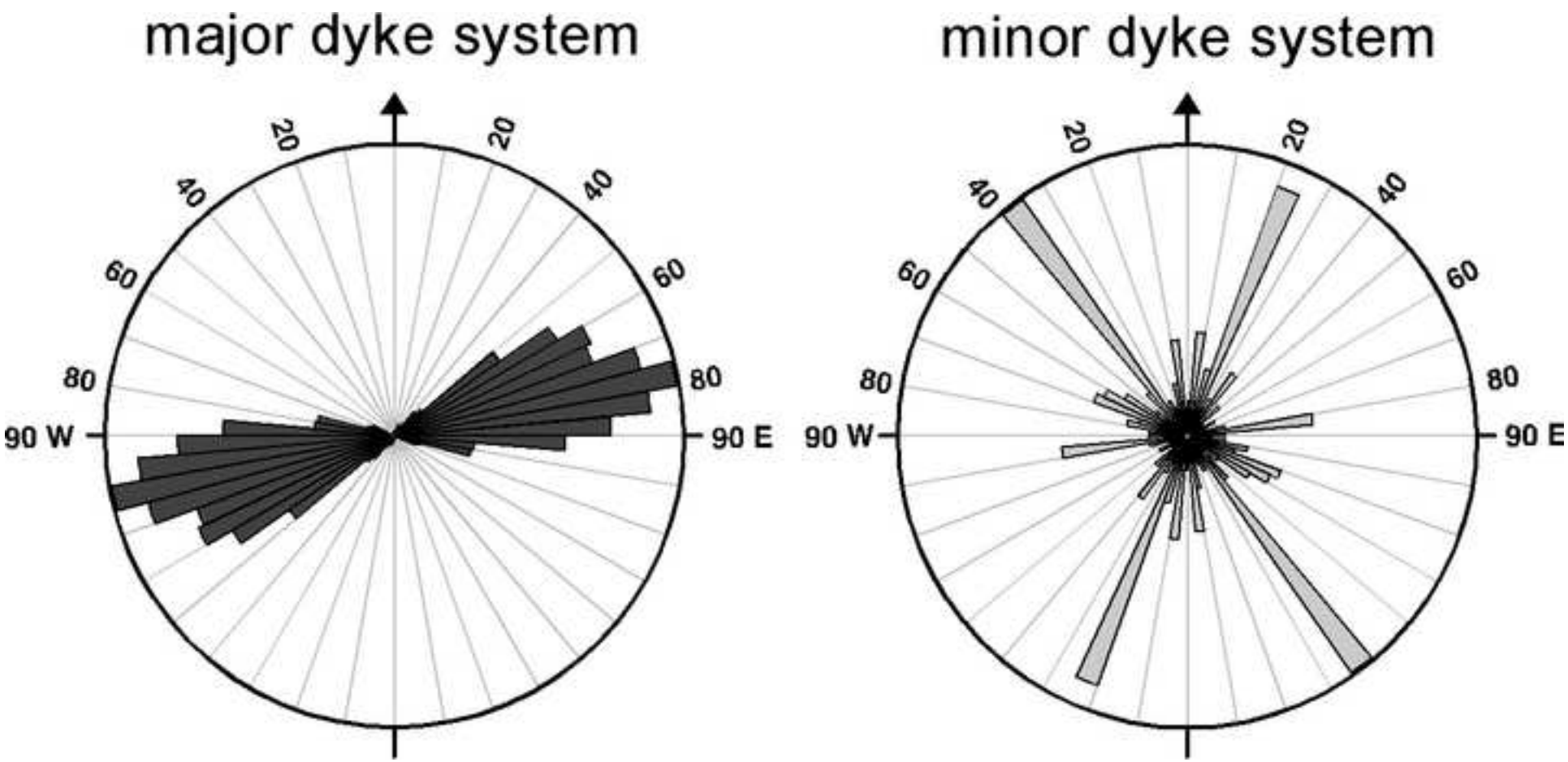

Figure 12

Click here to download high resolution image

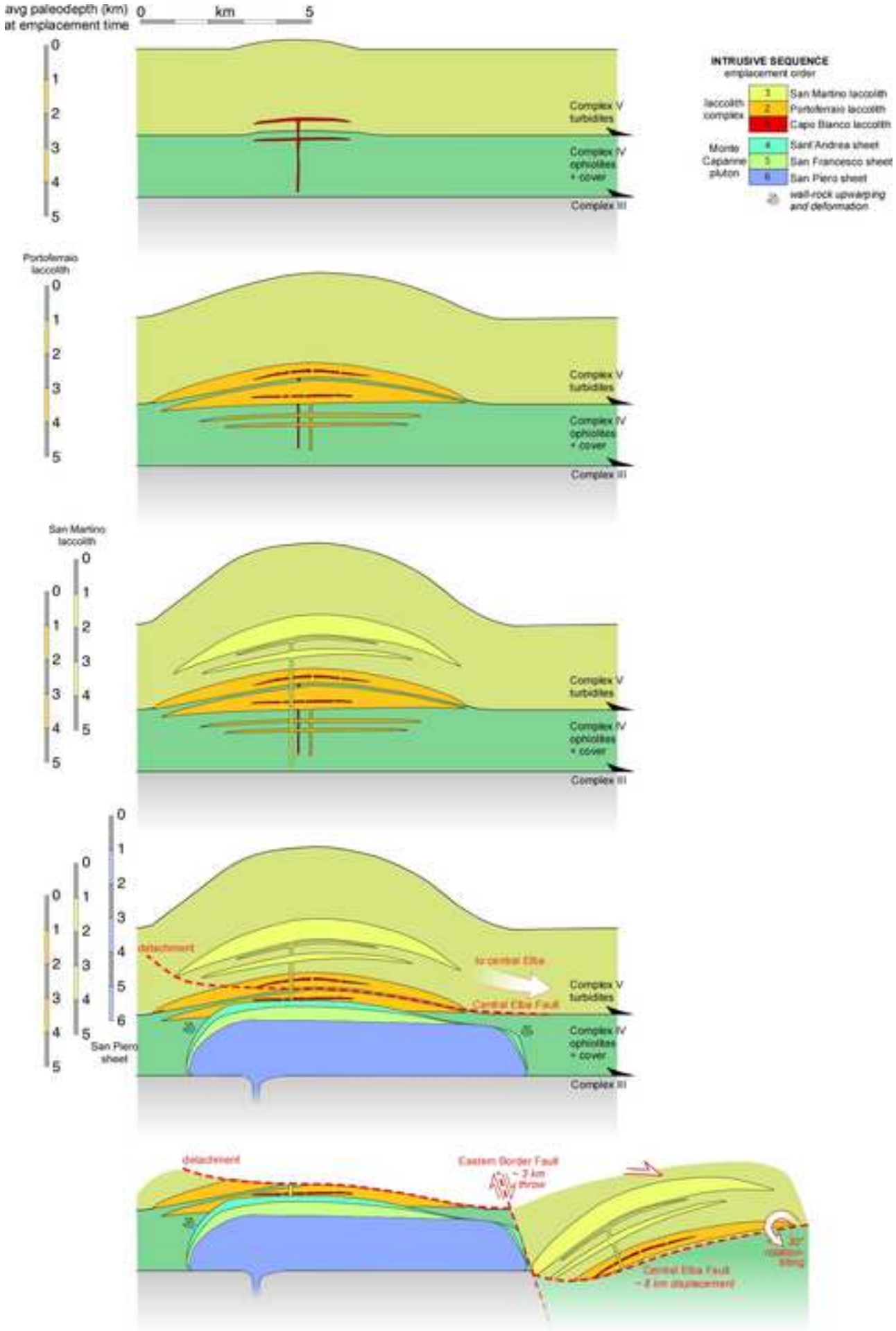

Figure 13
Click here to download high resolution image

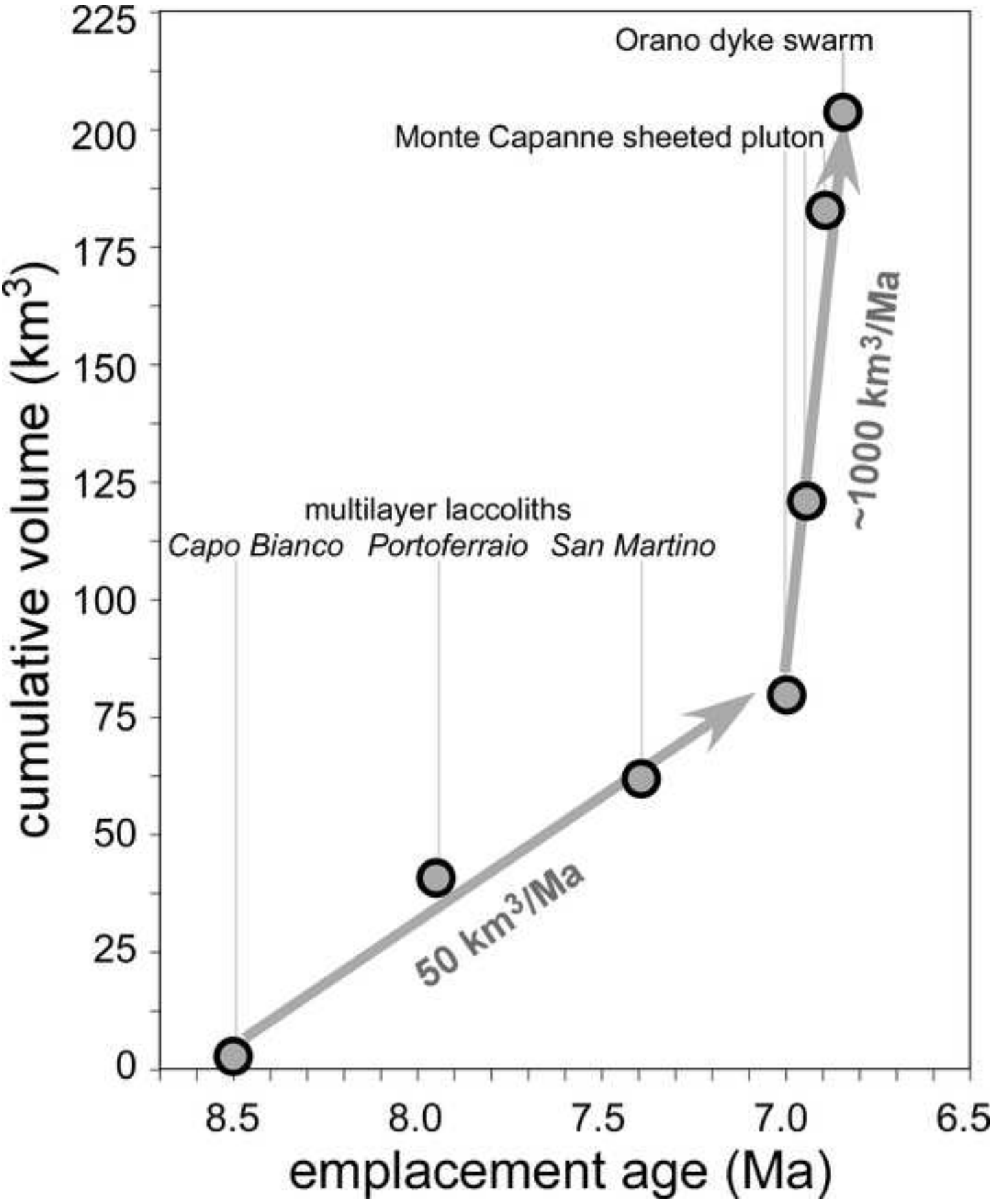

Dear Editor,

We revised the paper "Rise and fall of a multi-sheet intrusive complex, Elba Island, Italy" according to the reviews provided.
We are addressing each point raised in the reviews separately, as specifically reported below.
We would like to thank the Reviewers for thair suggestions

Best regards,
the corresponding Author, Sergio Rocchi

Reviewer #1

… presentation of the estimated volumes of each component magma pulse, to the extent such estimates are possible. If the geochronological data allow for it, the authors could then quantitatively discuss variation in rates of magmatism throughout the history of the magmatic center.
At this stage we can envision the rates of magmatism considering each multilayer laccolith as a single pulse (we've no evidence for differential timing of emplacement for the different layers) and considering the Monte Capanne pluton as emplaced in three different moments, separated from each other by time intervals of the order of ka (Farina et al, 2010). More precise evaluations could be done after the data presented at the recent GSA meeting by Barboni et al. will be published.

Section 2.2.1a., lines 17-20: I think I would be satisfied with the addition of a couple of words noting the presence of an inferred divergent flow field, a la Paterson et al., 1995. Interpreting magmatic fabric patterns in plutons. Lithos, 44: 53-82.
Done (1998).

Section 3.2.2., lines 40-44: It would be helpful to describe briefly the process through which Hogan and Gilbert (1995) envision reduction of the horizontal stress magnitude through an increase in the rate of magma supply.
Noted that increase supply increases dilational stress – the rest of the reasoning follows from the formula for calculating magma driving pressure.

Section 4.2., line 17: It would be helpful to mention briefly in section 4.1. that the dyke magmas are derived from mantle melting (or so I assume, based on the text here).
… mantle-derived lamproitic magma (Dini et al., 2002), … added.

Section 5.1.: ... I am a bit skeptical of the estimates of surface slopes developed during evolution of the magmatic center at depth. ...
The phrase "to the extreme" was removed.

** Figure comments **
Fig. 12: Portoferraio is misspelled in the legend.

Fixed.

Reviewer #2

Some of these comments are provocative, but, since I also work in subvolcanic systems, I know that there might be no answer to all of these. If so, it should be admitted.

1. What about 8- 6.8 Ma volcanoclastics, potentially equivalent to the Elba-Complex evolution, drilled by ODP/IODP in the northern Tyrrhenian Sea: Evidence of possible accompanying volcanism?

To our knowledge, the DSDP/ODP/IODP holes in the Tyrrhenian Sea are all located in younger (Pliocene) oceanic crust of the southern Tyrrhenian Sea, and no holes have been drilled in the shallow waters of the northen Tyrrhenian sea, where late Miocene clastic deposits could have been preserved. Only dredged samples comes from there. Only one known volcaniclastic material with an age of 7.4 Ma crop out on mainland Tuscany: this is now commented in Sect 2.4.

2. I suggest to rename headings: ...

Revised as requested.

3. What are the constraints for the temporal succession of the Elba laccolith complexes: radiometric ages or cross cut field relations? If it is the former, we need ages with error ranges. Please state and evaluate this somewhere!

It is now noted in the Introduction that the relative chronology in western–central Elba has been firmly established on the basis of crosscutting relations. Also noted is that reported absolute ages are consistent with the relative chronology constrained by field relations.

4. On pages 6 and 7, and in Chapter 6: A laccolith is nothing failed:

Appropriate phrases have been inserted to clarify that it is well understood that we are not suggesting that a Christmas tree geometry, once initiated, can evolve to an amalgamated pluton.

5. For the radiometric ages given in text and figures error ranges should be given!

We don't think this is realistic for this paper because the dates come from all kinds of different lines of evidence and reasoning. The responsibility will need to rest with the reader to obtain the details from references provided.

From Reviewer #2's pdf comments:

P1. Title:

Changed to "**Rise and fall of a multi-sheet intrusive complex, Elba Island, Italy**"

P1L15: Insert a paragraph at the beginning of Chapter 1, in which you set the stage for the Elba subvolcanic complex in the context of the state-of-the-art knowledge on subvolcanic systems world-wide. Do you know of other comparable Christmas Tree complexes?

The whole book is devoted to present such an overview, so it's better to avoid any duplication.

P1L31: Jurassic – middle spaces fixed.
P1L40-41: wording on “melted” repaired to: “became partially molten by decompression”
P1L50: reference to Serri et al. (1993) included.
P1L59: space inserted
P2L32: “throat clearing” replaced by : … the crust “breaking a sweat” of anatectic melt…
P2L40: fig 3a omitted.
P2L53: 3e not included; it’s not porphyry
P2L55: notation of eastward translation deleted replaced by simply noting that the main horizons are currently located in central Elba.
P2L56-57: laccolith dimension reconstruction referenced back to Rocchi et al. (2002).
P3L11: sentence split as suggested
P3L16: I assume, 2.2.1 is a very condensed summary of Roni et al. Why don't you take the time to explain to the reader carefully these important findings. Of course you should not double the Roni et al. paper.
Each section is essentially a very condensed summary of a previous, or in this case concurrent(?), paper. We think that this paragraph encapsulates the findings, and that readers can used the Roni paper as a source for more expanded explanations.

P3L45: Suggestion to change headers accepted.

P3L59-60: In Fig. 8 Pm (magma pressure) is featured, why not here in the text?
We think it is sufficient to address this in the figure caption, and have now done so.

P4L5-6: The fact that your laccolith sheets experienced vertical inflation, for me, is a sign that viscosity was important. Otherwise the sheets would have a lower aspect ratio.
This is not an issue relating viscosity and aspect ratio, which is obviously important for extrusive settings. We are not aware of any papers concerning this link in intrusive or subvolcanic settings.

P4L17-18: ok, but what about the orientation of the extensional stress? Fig. 6 suggests an E-W orientation of the feeder dyke. Was the tectonic extension oriented N-S during those days?
The possible persistence of the field is now noted in the dyke section P7.

P4L28-29: ok, but why the magma emplaced in more than one sheet? Can you comment on that?
Some phrases have been added in this section to clarify the concept that when the conditions were achieved for magma to flow horizontally, that traps were readily available in the zone where those conditions were met.

P4L35-36: Any thoughts about the emplacement succession of laccolith sheets within a given complex?
Now noted P2L58 that emplacement sequences for Christmas tree structures are unresolved.

P4L49-50: That is odd. What happened to the contacts, annealed? I guess it is not an outcrop problem.

Now noted that the absence is of “mappable” contacts. The basis for their identification has been detailed in Farina et al. (2010).

P5L11-12: Ref. Fig. 7: How did you estimate the depth of the base of the pluton? Is it exposed? The Complex IV is overlying, according to Fig. 4! Comment on this!
Estimate for pluton thickness now noted earlier, based on Dini et al. (2008). I don’t understand the issue of the position of Complex IV; the pluton intruded into Complex IV.

P5L18: Cruden and McCaffrey, 2002 added

P5L20: You cannot get rid of the intercalating host rock between the laccolith sheets.
Wording revised avoid any misunderstanding.

P5L28: How do you know that it was the first (in terms of time)? Or did I overlooked something?
The basis for the sequence of facies is the model of underplating developed by Farina et al. (2010). Arguments are inserted now in a previous section.

P5L45: this "legend" goes into the figure! Done

P6L6: Awkward phrasing revised.

P6L18: reference corrected to Dini et al., (2002)

P6L32: Suggested word change accepted to “take-home”

P6L37: See my comment on page 6. There is no evolution from Christmas to pluton! And see general comment no. 4.
Phrases added to clarify that Monte Capanne was “successful” because it exploited traps of its own making, while the Christmas trees exploited pre-existing structural traps, and thus “failed” to form plutons.

P6L49-51:
1. “… at 6.85 Ma ….” Corrected.
2. “Still mushy” character of MC pluton moved to after the abundant xenocryst evidence.
3. Covering laccolith layers retained; no evidence they were not already cooled.
4. The question of whether Orano dikes occur in eastern Elba has not been definitively answered. Nevertheless, one of three known outcrops has been dated at 5.83±0.14 Ma, thus ruling out a link with Orano dikes, which are 1 Ma older.

P6L57: Any constraints on the flow direction within the dykes: vertical, oblique, horizontal?
No constraints are available on Orano dikes.

P7L3: We have no constraints on age relations between major and minor dike sets.

P7L7-8: The orientation of the corresponding stress regime is similar to the one controlling the orientation of the laccolith-feeding dykes. Worth mentioning?

Sentence added noting the apparent persistence of an overall N-S extensional stress field from San Martino time through Orano time.

P8L8: I don't get the sense of this last sentence part. Maybe rephrase!?
Rephrased.

P8L60: I don't think the source of map is needed since it's our work.
P9L15: scale note moved as indicated.
P9L23: Fig 4 source: I don't think the source is needed since it's our work.
P9L28: Fig 5: scale noted
P9 Fig 6: corrected made as suggested.
P9 Fig 7: References noted in caption.
P9 Fig 8: Dashed line explained.
P9 Fig 9: Corrected as indicated.
P10 Fig 10: (PP) added.
P10 Fig 11: ~9,000 strike values explained.
P10 Fig 12: Addition of current land surface requested. Problematic, since this is a schematic section.